Submitted to Proceedings of the 4th International Planetary Probe Workshop, Pasadena, CA, June 25-29, 2006

FIELD TESTING AND DYNAMIC MODEL DEVELOPMENT FOR A MARS TUMBLEWEED ROVER*

R. Lorenz[1,3], A.Behar[2], F. Nicaise[2], J.Jonsson[2], M. Myers[1],

[1]Lunar and Planetary Laboratory, University of Arizona, Tucson, AZ 85721, USA.
[2]Robotic Vehicles Group, NASA/Jet Propulsion Laboratory, M/S 107-102, 4800 Oak Grove Dr., Pasadena CA 91109, USA. (3) Now at : Space Department, Johns Hopkins University Applied Physics Lab, 11100 Johns Hopkins Rd., Laurel, MD 20723-6099. email: Ralph.lorenz@jhuapl.edu

ABSTRACT

We present field measurements of the mobility performance of a tumbleweed rover (an instrumented wind-blown sphere) at Willcox Playa, Arizona. Video and GPS data are used, with meteorological stations deployed close enough to correlate motion with the wind. In the thin boundary layer of a desert playa, the drag coefficient is determined to be <0.2. Rolling and bouncing motions are discussed, and the performance of sphere-mounted flexible solar panels is evaluated.

.

1. INTRODUCTION

A Tumbleweed rover [1,2,3,4] is a quasi-spherical vehicle intended to traverse a planetary surface (nominally Mars) with a rolling and/our bouncing motion driven by the wind, much as the 'tumbleweed' or Russian Thistle is driven across the desert (figure 1).

Figure 1. A terrestrial Tumbleweed, highly evolved for mobility. Note that barbed-wire fences are unlikely to be an obstacle on Mars.

* *This work was performed by the Jet Propulsion Laboratory, a division of California Institute of Technology, under contract to NASA.*

As such, its trajectory is largely uncontrollable, but it offers the potential for much longer range surveys than conventional rovers. Two origins have been cited for the concept – inspiration from the bouncing motion of Pathfinder during its airbag landing, and the rapid wind-blown movement of a spherical wheel that had been removed from a rover under test on a playa.

The conventional configuration (figure 2) is spherical by inflation, with an equipment package suspended in the center by tension cords, although we have also explored other arrangements (electronic equipment mounted on the spherical surface). Other workers have explored non-inflated concepts with rigid elements arranged to give a near-spherical shape such as the Dandelion and Kite (e.g. [5]).

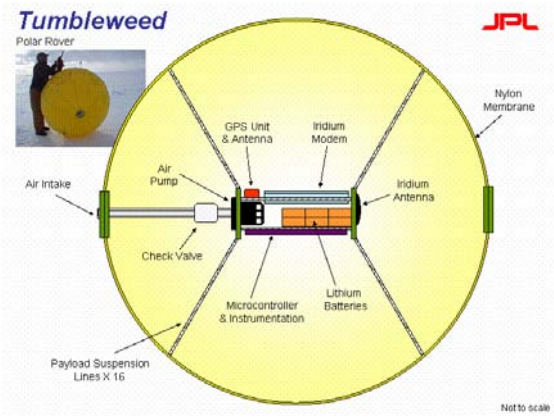

Figure 2. The Tumbleweed configuration used in field tests to date.

2. PRIOR FIELD TESTS AND RATIONALE FOR PRESENT WORK

Previously, several Tumbleweed rovers (e.g. [6]) have been deployed in polar regions, and have demonstrated a level of (unguided) mobility that surpasses that of conventional rovers by several orders of magnitude.

Deployment area, lifetime and distance travelled are as follows:

August 2003, Greenland, 9 days, 131 km
January 2004, South Pole, 7 days, 134 km
May 2004, Greenland, 7 days, 200km

These distances and times indicate an impressive average speed of ~0.3 m/s – almost a factor of 20 lower than the wind speed. Inspection of the GPS data (figure 3) shows that this is because the motion is strongly episodic – once the rover gets moving it moves quickly for a while, then stops, perhaps upon encountering an obstacle. (Additional deployments, not optimised for mobility evaluation, have included an air-drop deployment test in Antarctica.)

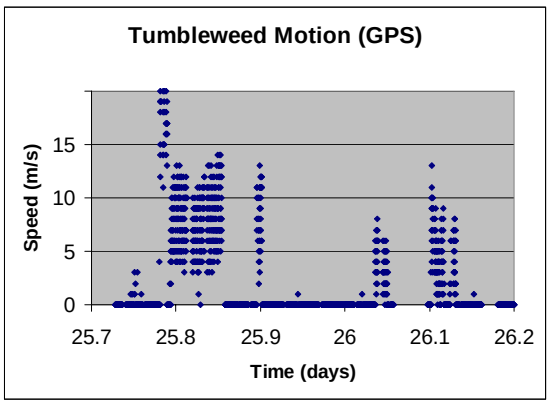

Figure 3. Part of the motion record of the South Pole tumbleweed rover from GPS data. The record is strongly intermittent, with periods of stasis interspersed with rapid movement.

It can be further seen (figure 4) that the episodic nature of the motion is not apparently due to the wind. Several factors confound the correlation of the launch site wind record and the motion history. First, the rover may respond to gusts of a duration too small to be captured in the low-time-resolution meteorological record (which is after all not acquired for this purpose). Second, as the rover moves away from the launch site, a lead or lag-time will be introduced – a gust front moving at, say, 5 m/s will take several hours to traverse the distance between the met station and the rover. Third, local variations in wind due to terrain blockage etc may occur, and slopes will also affect the motion directly. Finally, the inertia of the rover and the thresholding of the motion (perhaps relating to bouncing as well as rolling) introduce nonlinearities in the relation of instantaneous wind and motion speed. It is these issues that we aim to confront with the present tests.

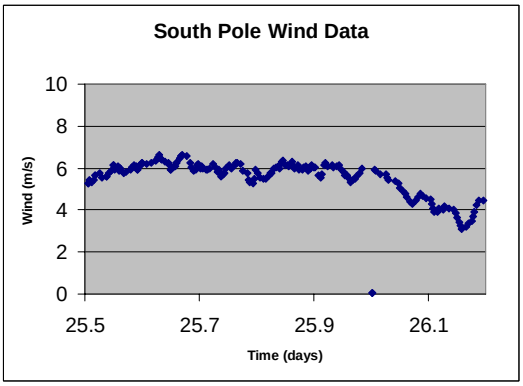

Figure 4. Wind measurements at the South pole, contemporaneous with the motion shown in figure 3. The winds are apparently much more steady than the motion record would indicate.

3. FIELD TESTS

3.1 Field Site

Field Tests were conducted at the Northwestern end of Willcox Playa in Eastern Arizona, about 1hr drive from the University of Arizona. Tests were conducted in February 2006. Our tests were conducted in the northwestern part managed by the Bureau of Land Management.

The site provides easy access, and a large area for rolling. It is of note that natural tumbleweed are found there in abundance.

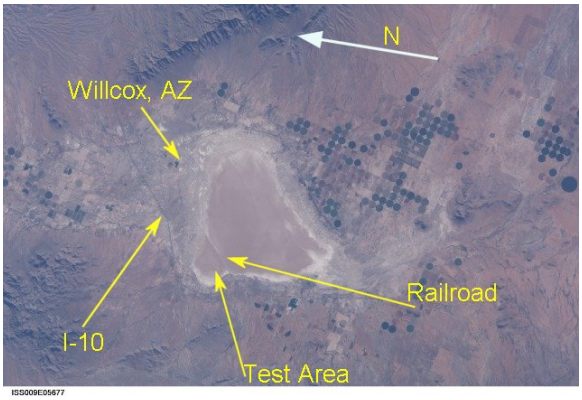

Figure 5. Annotated version of digital image from the International Space Station (image ISS009-E-5677 courtesy of http://eol.jsc.nasa.gov). The majority of the playa is used for military training and is not readily accessible.

3.2 Rover and Mass Properties

Figure 6. Rover in the field. Left to right are authors Nicaise, Behar, Lorenz and Jonsson.

The rover used in the field tests comprises a spherical shell of ballistic nylon with a diameter of 1.83m and a mass of 7.25kg. Its moment of inertia I is therefore 4.05 kgm^2. Suspended on a set of cords is a cylinder (35cm long by 16.5cm diameter) carrying the rover instrumentation and pumps. This cylinder, with a mass of 8.15kg, has axial and transverse moments of inertia of 0.03 and 0.09 kgm^2 respectively. Taking the two items together gives vary similar total moments of inertia of 4.08 and 4.15 kgm^2 - these are sufficiently close that there is no strong preference for axis of rotation : small deformations of the shell can cause larger deviations in I than this difference. Total mass m is 15.4 kg.

The moment of inertia is not negligible in the partitioning of energy between rotational and translational motions. If rolling without skid ($V=\omega R$, R=0.91m) then the translational kinetic energy ($0.5mV^2$) is $7.7V^2$, while the rotational kinetic energy $0.5I\omega^2 = 2.5V^2$ – or in other words the vehicle has ~30% more energy in total than can be attributed to translation alone.

3.3 Meteorological Measurements

We installed two meteorological monitoring instruments in the field, about 50m apart and close to the rolling area of the rover (in one case the rover collided with the monitor). First was a Davis anemometer and weathervane on a tripod, with data sampled by a microcontroller and stored on-board for later download. The second was a three-anemometer array, with anemometers at logarithmically-spaced heights to measure the thickness of the boundary layer.

Experience is such as to recommend as much redundancy in field measurements as is reasonably possible, to accommodate unanticipated effects and attrition in the field. A handheld anemometer was also used, and by reading the display aloud could be captured in the video record to facilitate timetagging. Wind noise on the video record (including a periodic flapping of the tethered wind cap) correlated with wind speed, although a quantitative calibration of this effect has not been attempted as yet.

The anemometer data (with a resolution of a few seconds) correlate well with each other, and thus may be expected to correlate well with the motion of the rover. Careful time-tagging is essential – notice that there is a ~10m periodicity in the windspeed (figure 7).

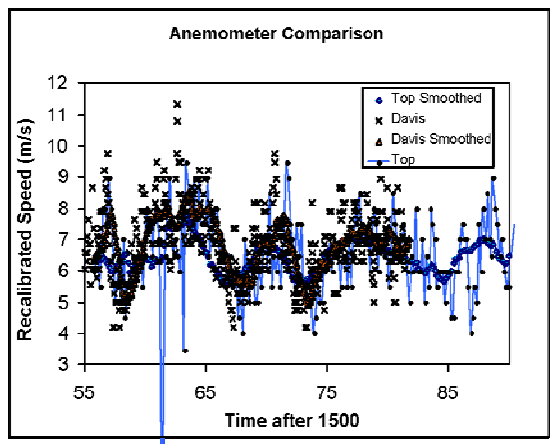

Figure 7. Anemometer records about 50m apart – good correlation is seen. Typical wind speed is ~6.5 m/s.

A plot of the windspeed versus logarithmic height (figure 8) permits a regression of the aerodynamic roughness length, which approximately corresponds to the scale of roughness of the surface. For the playa this is rather small – our data indicate ~0.5cm. (For comparison, the roughness measured the same way at the rocky Pathfinder landing site was some ten times larger. [7])

Thus, in the present experiment, the wind field experienced by the rover can be considered uniform – the boundary layer is so thin that there is only a small (~20%) variation in windspeed from the center of the rover to the top. In rougher environments this will not be the case, and the wind gradient may lead to several effects which may be rather important in influencing the rover's

motion – some aerodynamic lift may be generated, and the shear may cause a rolling moment that may assist the motion.

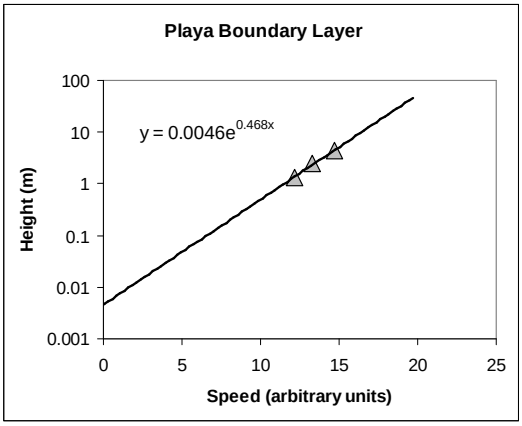

Figure 8. Windspeed vs height, indicating an aerodynamic roughness of only 0.5cm.

3.4 Video Measurements

Although GPS is ideal for large-scale motion studies, on very short timescales a more convenient tracking technique is to use video. A commercial camcorder was set up on a tripod and the onset of Tumbleweed motion was monitored. Video also permits documentation of effects such as whether the vehicle is rolling or bouncing. While the difference in accelerometer readings is very clear [8] between these two modes of travel when data is acquired at ~ 10 times a second, the instrumentation in our field deployments was not sampled as fast).

The video tape was digitized with a USB frame grabber. The resulting windows movie file (.wmv) was converted into a sequence of individual frames (.avi) with Videoconverter software. The .avi sequence was then analyzed with Videopoint software which creates an excel file of pixel positions by clicking a cursor on features to be tracked (this has been previously used by RL to monitor attitude motions of a parachute-borne model of the Huygens probe – [9]) In the fast rolling sequence (1626hrs) the 6ft Tumbleweed was 30 pixels across, yielding a pixel scale of ~6cm/pixel (the motion was essentially orthogonal to the line of sight so the pixel scale did not change). Once it began moving, the Tumbleweed crossed the field of view of the camera in about 15 seconds.

Figure 9. Screenshot from Videpoint software, showing manually-digitized locations in each frame – the acceleration towards the right is evident.

Several different tests were performed, over a period of two days. These include sequences of rolling and bouncing motion, although the latter have not been studied in much detail as yet.

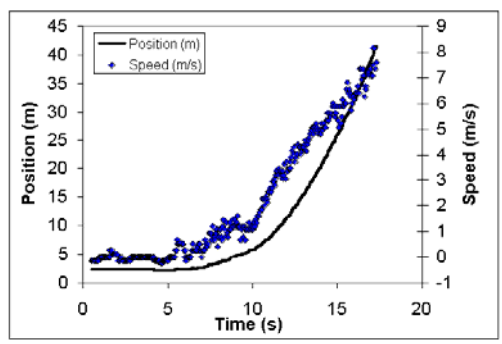

Figure 10. Position vs time, and velocity derived by differencing the positions at each frame step yielding a slightly noisy but high-time-resolution speed record.

It is evident from the appearance of the velocity plot as approximate line segments that there are two distinct phases – the first with a gentle acceleration of 0-1.2 m/s in the first 4.5 seconds of motion (an acceleration of 0.027g), while over the following 7 seconds the acceleration is much higher (0.09g), reaching 7.5 m/s. The speed determined by video agrees rather well with the GPS-determined speed (figure 11).

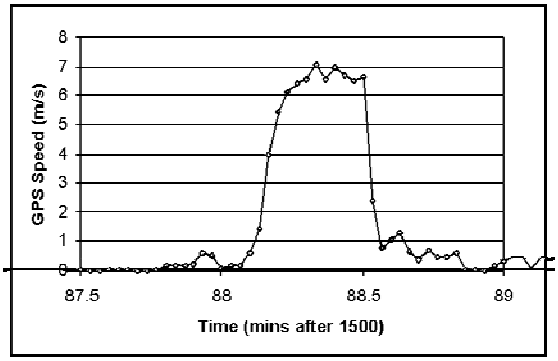

Figure 11. The Tumbleweed translation speed recorded by GPS. The steady-state speed is very close to the ambient windspeed, indicating very low rolling friction. The data have a much lower time resolution (~0.5s) than the video (0.04s).

4. DRAG COMPUTATION

The acceleration determined above allows the determination of the extraction of momentum from the wind to the rover i.e. the drag. If only translational motion is assumed, the drag on the tumbleweed must therefore be 4N and 13.6N. The anemometer record appears to indicate winds of 4-5 m/s rising to 9 m/s : the relative velocities would therefore be about 4-5 and 8 m/s respectively.

Taking the cross-section area as 2.6 m^2, and air density as 1.1 kg/m^3, (Willcox Playa is at 4100ft elevation) the drag coefficient for the faster phase of motion is therefore 0.14. However, if the vehicle is rolling without skid, as was apparent in the video, then the drag force coefficient must be augmented by 30% to account for the additional energy extracted from the airstream used to supply rotational kinetic energy – this correction yields C_d=0.19. The slower speed segment indicates a slightly smaller drag coefficient after rotation correction of C_d=0.14. In all cases these are lower limits, in that they do not account for any possible frictional losses.

At a flow speed of 2 m/s, the Reynolds number is 2.4×10^5, and the drag force on a smooth sphere would be expected to be of the order of 0.4 (e.g. see the Java C_d calculator at http://www.fluidmech.net/jscalc/cdre01.htm). At a flow speed of 7 m/s, the Reynolds number is 8.4×10^5 and the C_d, now in the turbulent regime, is only 0.1.

Thus the experimental results suggest a typical value between these two extremes, perhaps closer to the lower value of drag coefficient – not surprising given that the flow in the open air is likely to be somewhat turbulent.

Thus, following previous work [6], it seems probable that the performance of a Tumbleweed could be enhanced by drag augmentation devices on the surface, or an architecture like that of the natural Tumbleweed, where the flow in part goes through, not around, the plant [10].

5. SOME REMARKS ON BOUNCING

The onset of bouncing was clearly facilitated by the presence of surface roughness elements. However, once bouncing began, it often grew, suggesting bouncing may be a preferred mode of locomotion.

It was observed that the rover tended to bounce and rotate about a short axis of the central cylinder. This is obviously the axis of maximum moment of inertia, although some investigation of whether the position and tension of the suspension cords plays a role in defining the preferred spin axis would be worthwhile. The axis of maximum moment of inertia is of course the dynamically favoured (lowest energy) axis for spin.

Careful study of video records of bouncing (e.g. figure 12) shows an unexpected effect – the vehicle tends to spin forwards at a rate such that it bounces exactly twice per rotation (i.e. it bounces repeatedly on two opposite points on the sphere). Again, whether this is a purely dynamical effect, or is influenced by cord tension or friction effects would be worth exploring.

Figure 12. Action shot of the rover bouncing (note the shadow) The plane of rotation is roughly in the image plane – the short axis of the spheroid is the long axis of the internal cylinder and thus the axis of maximum moment of inertia.

In one sense, bouncing is an inefficient mode of transport, in that without roll, the vehicle experiences friction during the contact phases of bouncing, whereas in pure roll, there is no relative motion and thus no friction. However, the friction tends to promote rolling, leading to the combined bounce/roll described above.

In a thin boundary layer, this may be the end of the (simple) story. However, in a thick boundary layer with a significant wind gradient with height, bouncing may allow the rover to access faster winds above the ground.

Clearly, future work should consider, model and perhaps optimize, the bouncing performance of a vehicle of this type.

6. MOTION THRESHOLD

We measured the windspeed at which our rover began to move. This threshold of course depends on the level of inflation – to begin rolling, the net force of wind drag and weight (minus lift, if any) must be sufficiently forward of the central contact point to cause a net moment.

At rest, the internal pressure excess of the ball, multiplied by the contact area, will equal the weight: as the inflation pressure is decreased, the contact area increases, and thus the drag force and wind speed required to initiate motion will increase. The influence of inflation pressure on rolling/bouncing performance is of course well-known to soccer players. The data we obtained indicates an approximately inverse relationship between threshold wind speed and the inflation pressure (see table 1 below).

Level of inflation %	Wind speed m/s
100	4.5
80	5.5
70	7.0
50	9.5

Table 1. Rolling threshold wind speed as a function of inflation.

7. SURFACE-MOUNTED FLEXIBLE SOLAR CELLS

Until now, Tumbleweed rovers have been purely battery powered. In order to achieve a mission duration in excess of a few days, an alternative power source is required, with solar power being an obvious choice. Traditional crystalline cells are fragile, but amorphous silicon cells are now available which are fabricated onto a flexible substrate. Here we show a proof-of-concept experiment on the ability of such cells to develop power even after rolling in a dusty environment.

A thin-film solar cell was installed on the side of a PVC sphere (figure 13). The short-circuit current was measured aiming the cell at the sun. The sphere was then kicked around on a dusty field to simulate windblown rolling and bouncing and the short-circuit current measured after 10,30,100 and 300m of travel. It was noted that while the cell became somewhat dusty after a very short interval, the dustiness did not increase – soon the rate of dust removal by abrasion matches the rate of dust accumulation and a near-steady state is reached.

Figure 13. Tefzel-coated solar cell at start (above) and after 300m of rolling (below).

The short-circuit currents (and thus the power outputs) stabilized at about 70% of the dust-free case (figure 14). There was no obvious difference in dust obscuration for a cell coated with a cellulose tape and one with a UV- abrasion-resistant Tefzel coat, although something like the

latter would probably be preferred for long-duration use.

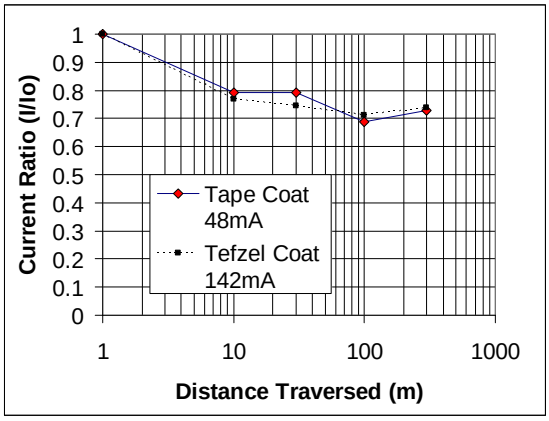

Figure 14. Short circuit current performance of flexible array as a function of distance traversed over a rough surface.

This experiment shows promise that an effective vehicle could use lightweight solar cells on its perimeter to provide power in all orientations. The large area available means that even with the modest loss in capacity due to dust obscuration ample power to support science measurements and data return.

8. CONCLUSIONS

Study of GPS data from polar field deployments suggests a poor correlation of the motion of a Tumbleweed rover with the meteorological record from the launch site. The motion is strongly episodic, suggesting the influence of short-period variations in windspeed and threshold effects on motion.

A short program of field tests with on-site documentation of the winds have permitted the quantitative measurement of the drag and rolling performance. As expected, the drag coefficient is rather low and could be improved.

Close observation of the motion in real-world conditions indicates some aspects of the bouncing motion (which may be the dominant mode of travel) which may allow rather superior performance than pure rolling.

Future work should explore this motion in more detail, and investigate the performance of a rover on terrain with a larger aerodynamic roughness.

Some simple tests show that flexible solar cells mounted on the exterior of a tumbleweed may be able to provide adequate power, dust accumulation becoming self-limiting after ~30% obscuration.

9. REFERENCES

1. G. Hajos, J. Jones and A. Behar, M. Dodd, An Overview of Wind-Driven Rovers for Planetary Exploration, AIAA-2005-0244, 43rd AIAA Aerospace Sciences Meeting and Exhibit, Reno, Nevada, Jan. 10-13, 2005

2. J. A. Jones, Inflatable Robotics for Planetary Applications, 6th International Symposium on Artifical Intelligence, Robotics and Automation in Space I-SAIRAS, Montreal, Canada, June 19-21, 2001.

3. J. Antol, Philip Calhoun, John Flick, Gregory A. Hajos, Richard Kolacinski, David Minton, Rachel Owens and Jennifer Parker, Low Cost Mars Surface Exploration: The Mars Tumbleweed, NASA/TM-2003 212411, August 2003 – see also http://centauri.larc.nasa.gov/tumbleweed/

4. Lorenz, R D, J Jones and J Wu, Mars Magnetometry from a Tumbleweed Rover, IEEEAC paper #1054, IEEE Aerospace Conference, Big Sky Montana, March 2003

5. S. Rose, C. Moody, D. James, and A. Barhorst, Drag Measurement and Dynamic Simulation of Martian Wind Driven Sensor Platform Concepts, AIAA-2005-249, 43rd AIAA Aerospace Sciences Meeting and Exhibit, Reno, Nevada, Jan. 10-13, 2005

6. A. Behar, F.rank Carsey, J. Matthews, J. Jones, NASA/JPL Tumbleweed Polar Rover, IEEE Aerospace Conference, Big Sky Montana, March 2004 – see also http://robotics.jpl.nasa.gov/ ~behar/JPLTumbleweed.html

7. Sullivan, R. et al., Results of the Imager for Mars Pathfinder windsock experiment, Journal of Geophysical Research Vol. 105, (E10), pp. 24,547–24,562, 2000

8. R. D Lorenz, Miniaturized Testbeds for Planetary Probes : Tumbleweed and Frisbee, IEEE Aerospace Conference, Big Sky, Montana, March 2005

9. R D Lorenz, J M Dooley and K Brock, Dynamics and Measurements of a Scale-Model

Huygens Probe parachute-dropped from a model aircraft, 3rd International Planetary Probe Workshop, Anavyssos, Greece, June 2005

10. R. D. Lorenz, Spinning Flight : Dynamics of Frisbees, Boomerangs, Samaras and Skipping Stones, Copernicus-Springer, 2006

10. ACKNOWLEDGEMENTS

The authors acknowledge the support of a JPL DRDF grant.